Reports of Biochemistry & Molecular Biology
Vol.11, No.4, Jan 2023

Original article

www.RBMB.net

Sodium Hydrosulfide Modification of Mesenchymal Stem Cell-Exosomes Improves Liver Function in CCL4-Induced Hepatic Injury in Mice

Maryam Jafar Sameri*[1,2], Rafeie Belali[1], Niloofar Neisi[3], Reza Noei Razliqi*[1], Seyed Ali Mard[4], Feryal Savari[5], Seyyed Saeed Azandeh[6]

Abstract

Background: Liver diseases and injuries are important medical problems worldwide. Acute liver failure (ALF) is a clinical syndrome characterized by severe functional impairment and widespread death of hepatocytes. Liver transplantation is the only treatment available so far. Exosomes are nanovesicles originating from intracellular organelles. They regulate the cellular and molecular mechanisms of their recipient cells and have promising potential for clinical application in acute and chronic liver injuries. This study compares the effect of Sodium hydrosulfide (NaHS) modified exosomes with non-modified exosomes in CCL4-induced acute liver injury to ascertain their role in ameliorating hepatic injury.

Methods: Human Mesenchymal stem cells (MSCs) were treated with or without NaHS (1 µmol) and exosomes were isolated using an exosome isolation kit. Male mice (8-12 weeks old) were randomly divided into four groups (n=6): 1-control, 2-PBS, 3- MSC-Exo, and 4- H2S-Exo. Animals received 2.8 ml/kg body weight of CCL4 solution intraperitoneally, and 24 h later MSC-Exo (non-modified), H2S-Exo (NaHS-modified), or PBS, was injected in the tail vein. Moreover, 24 h after Exo administration, mice were sacrificed for tissue and blood collection.

Results: Administration of both MSC-Exo and H2S-Exo reduced inflammatory cytokines (IL-6, TNF-α), total oxidant levels, liver aminotransferases, and cellular apoptosis.

Conclusions: MSC-Exo and H2S-Exo had hepato-protective effects against CCL4-induced liver injury in mice. Modification of cell culture medium with NaHS as an H2S donor enhances the therapeutic effects of MSC exosomes.

Keywords: Acute liver failure (ALF), CCL4-induced liver injury, Exosomes, Mesenchymal stem cells (MSCs), Sodium hydrosulfide (NaHS).

Introduction

Liver diseases and injuries are important medical problems worldwide. Acute liver failure (ALF) is a clinical syndrome characterized by severe functional

1: Student Research Committee, Ahvaz Jundishapur University of Medical Sciences, Ahvaz, Iran.
2: Physiology department, Abadan University of Medical Sciences, Abadan, Iran.
3: Infectious and Tropical Diseases Research Center, Health Research Institute, Department of Medical virology, School of Medicine, Ahvaz Jundishapur University of Medical Sciences, Ahvaz, Iran.
4: Persian Gulf Physiology Research Center, Medical Basic Sciences Research Institute, Ahvaz Jundishapur University of Medical Sciences, Ahvaz, Iran.
5: Department of basic sciences, Shoushtar Faculty of Medical Sciences, Shoushtar, Iran.
6: Department of Anatomical Sciences, School of Medicine, Cellular and Molecular Research Center, Ahvaz Jundishapur University of Medical Sciences, Ahvaz, Iran.
***Corresponding author: Maryam Jafar Sameri; Tel: +98 9381267697; E-mail: M.Jafarsameri@Abadanums.ac.ir**
& Reza Noei Razliqi; Tel: +98 9381267697; E-mail: noei.r@ajums.ac.ir.
Received: 19 Oct, 2022; Accepted: 22 Oct, 2022

impairment and widespread death of hepatocytes. The mortality rate is close to 80%, and liver transplantation is the only treatment available so far (1). The main cause is viral infections and in many countries hepatitis A, B, and E are recognized as the main causes of this disease (2). Activation of liver innate immunity leads to acute damage. Despite the secretion of chemokines by immune cells, their primary secretion source is hepatocytes, Kupffer cells, stellate cells, sinusoidal cells, endothelial cells, and biliary epithelial cells (3). Kupffer cells are highly effective in diminishing and eliminating pathogenic agents, but they also cause additional tissue damage by recruitment of immune cells, secretion of toxic compounds such as proteases, and production of reactive oxygen species (ROS) (4). Released chemokines and inflammatory cytokines activate the NFκB pathway, which in turn, accompanies TNF-α production in hepatocytes (5). Produced ROS and increased levels of TNF-α have cytotoxicity effects to hepatocytes, bringing about cell death (6, 7).

Exosomes are nanovesicles, ranging from 30 to 200 nm, that originate from the intracellular organelles and are released from various cell types (8). Recently, much attention has been paid to Mesenchymal stem cells (MSC) exosomes as therapeutic applications.

Numerous strategies have been defined to enhance stem cell efficacy, including preconditioning, genetic modification, and optimization of MSC culture conditions (9-11). Preconditioning of MSCs by hypoxia, pharmacological agents, chemical agents, trophic factors, cytokines, and physical factors directly influence their paracrine effects and improve exosome regulatory function on the inflammatory factors (12, 13). Exogenous Hydrogen sulfide (H2S) proceeds as a powerful signaling molecule that exerts cytoprotective, anti-inflammatory, antioxidant, and anti-apoptotic effects in chronic and acute liver inflammation and hepatic ischemia-reperfusion injury (14-16). It has been reported that H2S-modified extracellular vesicles (EVs) reduce inflammatory cytokines and enhance the therapeutic effects of MSC-EVs in brain ischemia-reperfusion (17).

In the present study, we evaluated sodium hydrosulfide (NaHS) preconditioned MSC exosomes, an H2S donor, on CCL4-induced acute liver injury to ascertain their role in ameliorating hepatic injury.

Materials and Methods

Cell culture, exosome isolation, and NaHS treatment

Human umbilical cord bone marrow-derived MSC were purchased from Bon Yakhteh Research Center (Tehran, Iran) and were cultured in high glucose Dulbecco's modified Eagle medium (DMEM) supplemented with 10% fetal bovine serum (FBS) and incubated in 95% room air, 5% dioxide at 37 °C. All media was obtained from BIO-IDEA (Tehran, Iran).

Menchymal stem cells (MSCs) were cultured in a 75 ml flask, and the culture media was changed to a serum-free medium after three phosphate-buffered saline (PBS) washes when confluency reached nearly 80%. After three PBS washes, MSC was treated with NaHS for 48 hours (1 μmol concentration, based on our previous study (18) in an FBS-free medium to produce H2S conditioned Exo. Supernatants were stored at -80 °C until needed for the extracellular vesicle isolation procedure.

Exosome isolation procedures were carried out as follows: supernatants were centrifuged at 300 g for 10 minutes, 2000 g for 10 minutes, and finally 10 000 g for 10 minutes to remove dead cells and cell debris. The clarified supernatants were transferred to an Amicon 100 kDa Ultra15 centrifugal filter unit (Merck Millipore, USA) and centrifuged at 3000 g for 20 minutes. Finally, exosomes were extracted from the concentrated ultra-filter liquid using an exosome isolation kit (EXOCIB, Cib Biotech Co, Iran). Exosomes pellets resuspended in 200 microliters of cold PBS and were kept at -80 °C. To determine the protein content concentration of exosomes in

preparation for their potential use in future experiments on animals, the Bradford protein assay was carried out. Transmission electron microscopy and a western blot analysis of exosome markers (CD9 and CD63) were used to assess isolated exosomes.

Experimental animals

BALB/c male mice were provided from the animal center of Ahvaz Jundishapur University (Ahvaz, Iran). Animals were 8 to 12 weeks old and weighed 22 to 27 grams. All animals were kept in the laboratory of the Jundishapur University animal facility, with free access to laboratory food and water, at a temperature of 20 + 2 °C, and on a 12-hour light/dark cycle. All protocols were carried out in accordance with National Institutes of Health guidelines for the humane use of laboratory animals under the ethics committee of AJUMS (IR.AJUMS.ABHC.REC.1400.089).

Carbon tetrachloride (CCl4) solution was dissolved in pure corn oil at a 20% concentration one day before injection. Animals were randomly divided into four groups (N=6), 1-control, 2-CCL4 + PBS, 3-MSC-Exo, 4- H2S-Exo. The control mice received 1 ml/kg corn oil intraperitoneally. Other mice were injected with 2.8 ml/kg body weight of CCL4 solution (Merck, Germany) intraperitoneally, and after 24 h MSC-Exo (100 µg in 100 µl PBS), H2S-Exo (100 µg in 100 µl PBS) or phosphate-buffered saline (PBS), was injected in the tail vein. Moreover, 24 h after Exo administration, mice were sacrificed for tissue and blood collection.

Transmission electron microscopy

To prepare exosome samples for Transmission electron microscopy (TEM), Polanco and Scicluna's procedure was applied (19). On carbon-coated formvar film, we characterized exosomes using uranyl acetate negative staining. The exosome sample was fixed for 30 minutes with a 1:1 glutaraldehyde (2%) solution. Then, six µl of fixed exosomes were added to a 200 nm mesh copper grid with carbon-coated formvar film. After 10 minutes, the grid was briefly washed twice with 100 µl of MilliQ water and the excess liquid drained. The grid was placed on 30 µl of 1.5% uranyl acetate for 12 s and left to dry in the air after the excess liquid had been blotted away. The grid was observed under transmission electron microscopy at 80 to 100 kV.

Western blot

The frozen tissue lysed using lysing buffer (50 mM Tris,150 mM sodium chloride, 0.1% triton, sodium deoxycholate 0.25%, SDS 0.1%and EDTA were mixed in 20 ml of distilled water and its pH was set at 7.4. Protein concentrations were determined by the Bradford assay. Protein electrophoresis was performed using the SDS-PAGE method. The following steps were performed: The gel was placed in a transfer buffer for 10 to 15 minutes. A sandwich consisting of 5 layers, including two layers of sponge, two layers of Whatman paper on both sides, one layer of nitrocellulose paper, and one layer of gel, were prepared. After blocking the nitrocellulose membranes, washed three times with PBS for 5 minutes each time. Nitrocellulose membranes were incubated with the primary antibodies for an hour at room temperature and on a shaker at 65 g. These antibodies included cleaved caspase-3 antibody (rabbit monoclonal, Cell Signaling Technology, USA) and β-actin antibody (mouse monoclonal antibody, Santa Cruz Biotechnology, USA). Membranes were incubated for 90 minutes at room temperature with a Mouse polyclonal secondary antibody, M-IgGBP-HRP (Santa Cruz Biotechnology, USA), following five PBS washes. Each gene underwent bleaching on its own. The sensitive film and the membranes were housed in a plastic protective cassette, and the X-RAY processor produced the bands (LD-14, China). The expression of studied proteins was analyzed by JS 2000 device software and the values were normalized to b-actin. Primary mouse antibodies against CD9, CD63, TSG101 as ***a Housekeeping protein control were purchased from*** Santa Cruz Biotechnology, USA.

Cytokine Analysis

Hepatic tissues were assayed for TNF-α and IL-6 levels using enzyme-linked immunosorbent assay (ELISA) under the manufacturer's protocol (Karmania Pars Gene, Iran). The frozen tissue was lysed using RIPA lysing buffer, and samples or different concentrations of standards were added to a microplate pre-coated with a monoclonal antibody specific for mouse TNF-α and IL-6. After 3 times washing any unbound substances, a specific polyclonal antibody for mouse TNF-α and IL-6 was added to each well. After three times of washing, a substrate solution was added to the wells. After the enzyme reaction, the absorbance was measured using an ELISA reader (BioTek, USA) at 450 nm. concentrations of cytokines were obtained from the standard curve (20).

Real-time quantitative Polymerase Chain Reaction (RT-qPCR)

Hepatic tissue total RNA was extracted using an RNA extraction kit (RNeasy Mini Kit Qiagen, Germany) according to the manufacturer's instructions. Firstly, 30 mg of liver tissue was weighed and homogenized after adding 600 µl RLT buffer (WiseTis homogenizer, HG-15D, Witeg, Germany). Then After centrifugation of the lysate, cleared homogenate was moved to a new microtube, and ethanol (70%) was added. After three times washing, the purity and concentration of the extracted RNA were determined spectrophotometrically at 260 and 280 nm wavelengths (NanoDrop 2000; Thermo fisher scientific, USA).

Extracted total RNA was used for first-strand complementary DNA (cDNA) synthesizing (cDNA Synthesis kit, ANACELL, Iran). The cDNA samples were incubated at 70 °C for 5 min to stop the reaction. Quantitative PCR was performed using SYBR Green PCR Master Mix (High ROX; Amplicon, England) according to the protocol. Data expressed as fold increase over the control. The primers used are reported in Table 1.

Table 1. Real-Time PCR Specific Primers.

Gene	Forward (5-3)	Reverse (5-3)
BAK1	CAAGTGACGGTGGTCTCC	CTCCTGTTCCTGCTGGTG
BAX	TGAGGTTTATTGGCACCTCC	TTTTCCTGGATGAATGGGG
Bcl2	TGAGTACCTGAACCGGCATC	TAGTTCCACAAAGGCATCCCA
GAPDH	TGCTGGTGCTGAGTATGTCG	CGGAGATGATGACCCTTTG

BAK 1: Bcl2 Antagonist/Killer 1, **BAX:** Bcl-2-associated X protein, **Bcl2:** B-cell lymphoma 2, **GAPDH:** Glyceraldehyde-3-phosphate dehydrogenase.

Total Oxidant status

Tissue Total Oxidant Status (TOS) levels were estimated using a KTOS kit (Kiazist, Iran) according to the manufacturer's protocol. Briefly, 300 µl PBS buffer was added to 30 mg liver tissue and homogenized at 20000 × g for 5 minutes. After centrifugation at 12000 × g at 4 °C for 15 minutes, the supernatant was moved to a new microtube. A 50 µl-sample or different concentrations of standards were added to each well of a 96-well plate. Then, 200 µl substrate was added, and after 15 minutes, OD red at 560 nm. Concentration was calculated using the standard curve. Data normalized after that every sample protein concentration was measured by Bradford assay and expressed as nmol/mg protein (21).

Serum Biochemical Examination

The serum from the blood samples was transferred to a microtube and maintained at 20 °C after being centrifuged for 5 minutes at 12,000 g. On an Auto Chemistry Analyzer (BT-1500, Italy), in accordance with the kit's instructions (Pars Azmun, Tehran, Iran), the following enzymes were measured: aspartate aminotransferase (AST), alanine

aminotransferase (ALT), total bilirubin (T.Bili), and alkaline phosphatase (ALP) (22).

Histopathological Examination

Liver histological evaluation utilizing hematoxylin and eosin (H&E) staining was performed. Formalin-fixed liver tissue was sectioned at a thickness of 5 μm and placed in a tiny mold filled with melted paraffin. After being rehydrated with graded alcohol, sections were stained by hematoxylin and eosin (H & E). For histological evaluation, the Suzuki classification (sinusoidal congestion and vacuolization: None=0, Minimal=1, mild=2, moderate=3, severe=4, hepatocyte necrosis: None=0, single cell necrosis=1, 30%=2, 60%=3, 60%> 4) was utilized, and sections were graded from 0 to 4 (23).

Terminal dUTP nick-end labeling (TUNEL) assay

According to the manufacturer's instructions (Roche, China), sections were deparaffinized and submerged in methanol and H2O2 for 10 minutes. Proteinase was added for 30 minutes at 37 °C after three PBS washes. Sections were incubated in triton (0.3%) for 10 minutes and after 3 times washings, incubated for 2 hours in the presence of TdT, and DAB staining (ACV999-ScyTek, USA). Lastly, sections were imaged using an optical microscope (LABOMED, USA). The number of TUNEL-positive cells was counted and data were computed using the following formula: the number of apoptotic cells/total number of nucleated cells × 100% to assess the results in each slide (24).

Statistical analysis

Results are presented as means SD. The data were analyzed using one-way ANOVA and Tukey post hoc statistical testing. Kruskal-Wallis tests were used for nonparametric comparisons. Differences less than 0.05 were considered significant.

Results

Characterization of Exosomes

Transmission electron microscopy was used to confirm that exosome isolation was accurate. According to TEM images, exosomes showed a uniform pattern of spherical, nano-sized vesicles (Fig. 1B). Additionally, we utilized western blot analysis to assess the expression of the exosome-specific surface markers CD9 and CD63, and the results showed that exosome isolation was validated (Fig.1A).

MSC-Exo and H2S-Exo improve liver function of CCl4-induced liver injury

To evaluate the potential treatment ability of MSC-Exo and H2S-Exo on liver injury, serum levels of Alanine Transaminase (ALT), Aspartate Transaminase (AST), Total Bilirubin (T.Bili), and Alkaline Phosphatase (ALP) were measured using an autoanalyzer device. The serum levels of ALT, AST, T.Bili, and ALP increased significantly after CCL4 injection as compared to the control group. The administration of MSC-Exo and H2S-Exo decreased AST to, 133.66 and 89.50 (U/L), respectively, which was significant in comparison to the PBS group. MSC-Exo, and H2S-Exo treatment significantly decreased the ALT level in comparison to the PBS group. Importantly, H2S-Exo mice declined AST and ALT levels further that the MSC-Exo group, suggesting that H2S-modified MSC might improve the therapeutic ability of isolated exosomes (Figs. 1C and 1D).

Moreover, the T.Bili and ALP levels markedly decreased in MSC-Exo and H2S-Exo compared with those in the PBS group (Figs. 1E and 1F).

MSC-Exo and H2S-Exo attenuate the level of oxidant and inflammatory mediators in CCL4-induced liver injury mice

To investigate the effect of CCL4-induced liver injury on oxidant status and inflammatory cytokines, the total Oxidant, IL-6, and TNF-α levels were measured. The levels of oxidants in the PBS group were significantly higher than those of control mice. On the other hand, MSC-Exo and H2S-Exo administration reduced the level of TOS significantly compared to the PBS group (Fig. 2A).

Also, the results of this study showed a significant increase in IL-6 and TNF-α levels

following CCL4-induced liver injury (Figs. 2B and 2C). Treatment with MSC-Exo and H2S-Exo markedly, attenuated the IL-6 and TNF-α levels (Figs. 2B and 2C).

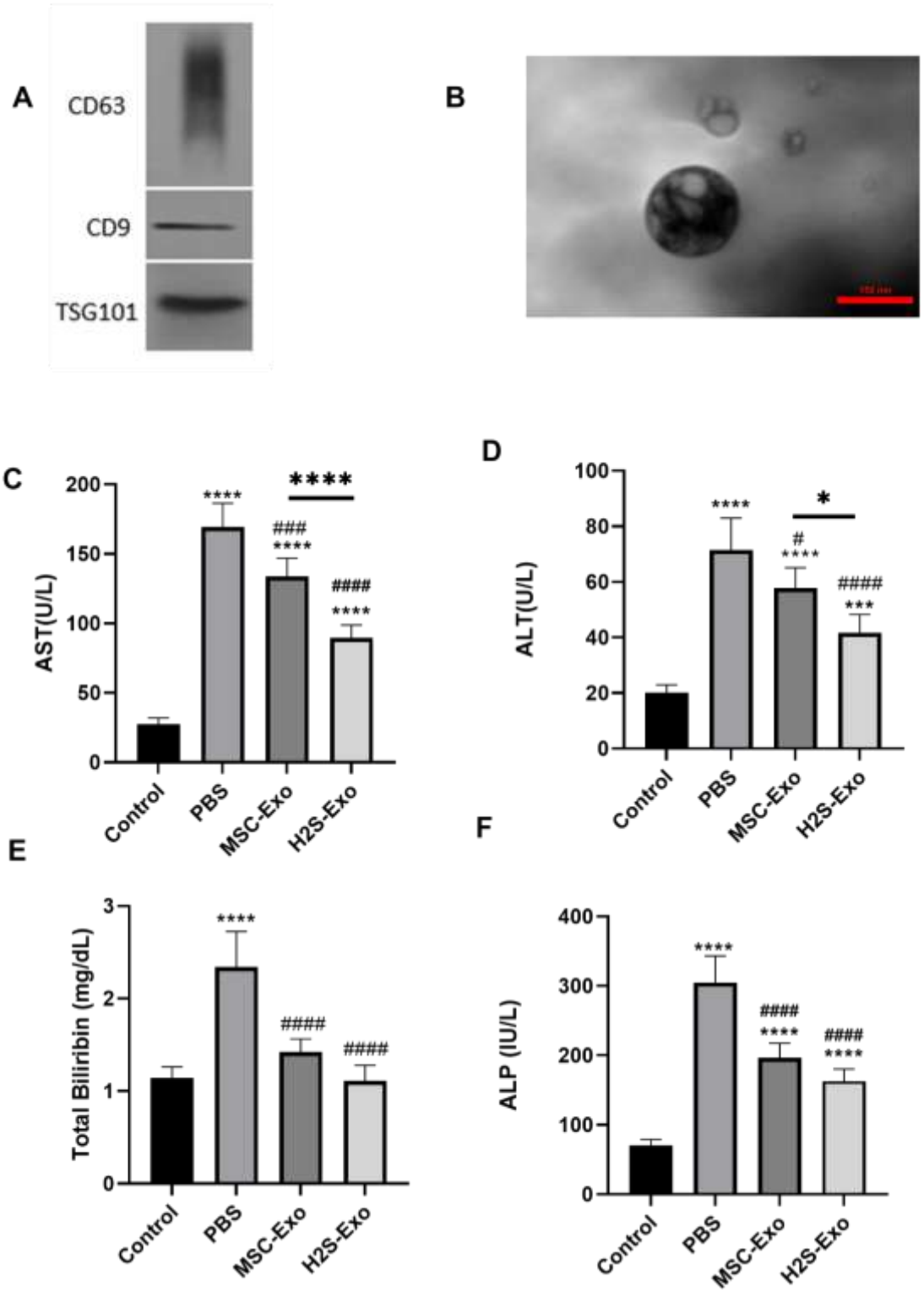

Fig. 1. Characterization of isolated exosomes and effect of MSC-Exo and H2S-Exo administration on liver aminotransferases in mice following CCL4-induced liver injury. (A) The specific vesicle-associated markers, CD63, CD9 and tsg101 were detected in MSC-Exosomes using Western blot analysis. (B) Representation of isolated exosomes transmission electron micrographs. (C) AST (Aspartate Aminotransferase); (D) ALT (Alanine Aminotransferase); (E) Total Bilirubin; (F) ALP (Alkaline Phosphatase). Mean ± SD. ***P<0.001, and ****P<0.0001 respectively compared to control. #P<0.05, ###P<0.001, and ####P<0.0001 compared to PBS.

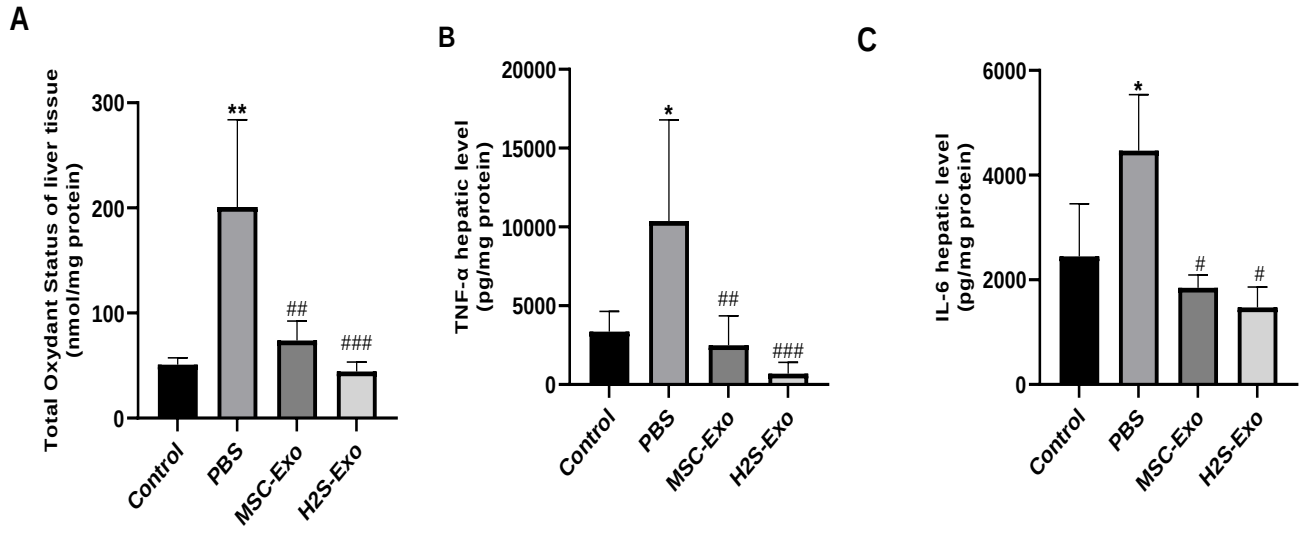

Fig. 2. Administration of MSC-Exo, and H2S-Exo attenuated the level of inflammatory mediators (TNF-α and IL-6) and TOS (total oxidant status) in CCL4-induced liver injury mice. Data expressed as mean± SD. *P<0.05 and **P<0.01 compared to the control group. #P<0.05, ##P<0.01, and ###P<0.001 compared to the PBS group.

MSC-Exo and H2S-Exo decline apoptosis

To clarify the effect of MSC-Exo and H2S-Exo on apoptotic genes and whether MSC-Exo and H2S-Exo treatment reduced liver apoptosis, the mRNA levels of BCL2 Antagonist/Killer 1 (BAK1), Bcl-2-associated X protein (BAX), and B-cell lymphoma 2 (BCL2) were measured using RT-PCR. The results of RT-PCR revealed that the mRNA levels of BAK1 and BAX were increased in the PBS group when compared to the control group (Fig. 3A and 3B). In contrast, the Bcl2 expression level was decreased in the PBS group notably in comparison to the control group (Fig. 3C).

Interestingly, MSC-Exo and H2S-Exo treatment attenuated the mRNA level of BAK1 significantly, and it was reversed completely. Moreover, the mRNA level of BAX, also, was decreased in MSC-Exo and H2S-Exo groups markedly (Figs. 3A and 3B). On the other hand, BCL2 was up-regulated in the H2S-Exo group compared to the PBS group. Interestingly, as shown in Fig. 3C no significant differences were seen in the MSC-Exo group compared to the PBS group (Fig. 3C).

We further investigated the protein level of cleaved caspase-3 and the TUNEL staining assay. As shown in Figs. 3D and E, aligned with the results of BAK1/BAX, the protein level of cleaved caspase-3 was elevated in the PBS group compared to those in the control, MSC-Exo, and H2S-Exo groups, which indicates the therapeutic effect of MSC-Exo and H2S-Exo in liver injury.

The livers from the control group's histological analysis revealed normal liver morphology, venules, and bile ducts, and no hepatocyte necrosis was found. The PBS group, on the other hand, showed architectural deformation, a loss of integrity, sinusoidal congestion, and a lightening of the cytoplasm of the hepatocytes with scattered necrosis. Groups treated with MSC-Exo and H2S-Exo reduced these morphological changes seen in the PBS group (Figs. 3F and 3G).

We also examined cell apoptosis in CCL4-induce liver injury mice using the TUNEL staining assay. Representative images and cell counting results showed that injection of MSC-Exo and H2S-Exo reduced TUNEL-positive cells to 20.40% and 19.74% respectively (Figs. 3G and 3H).

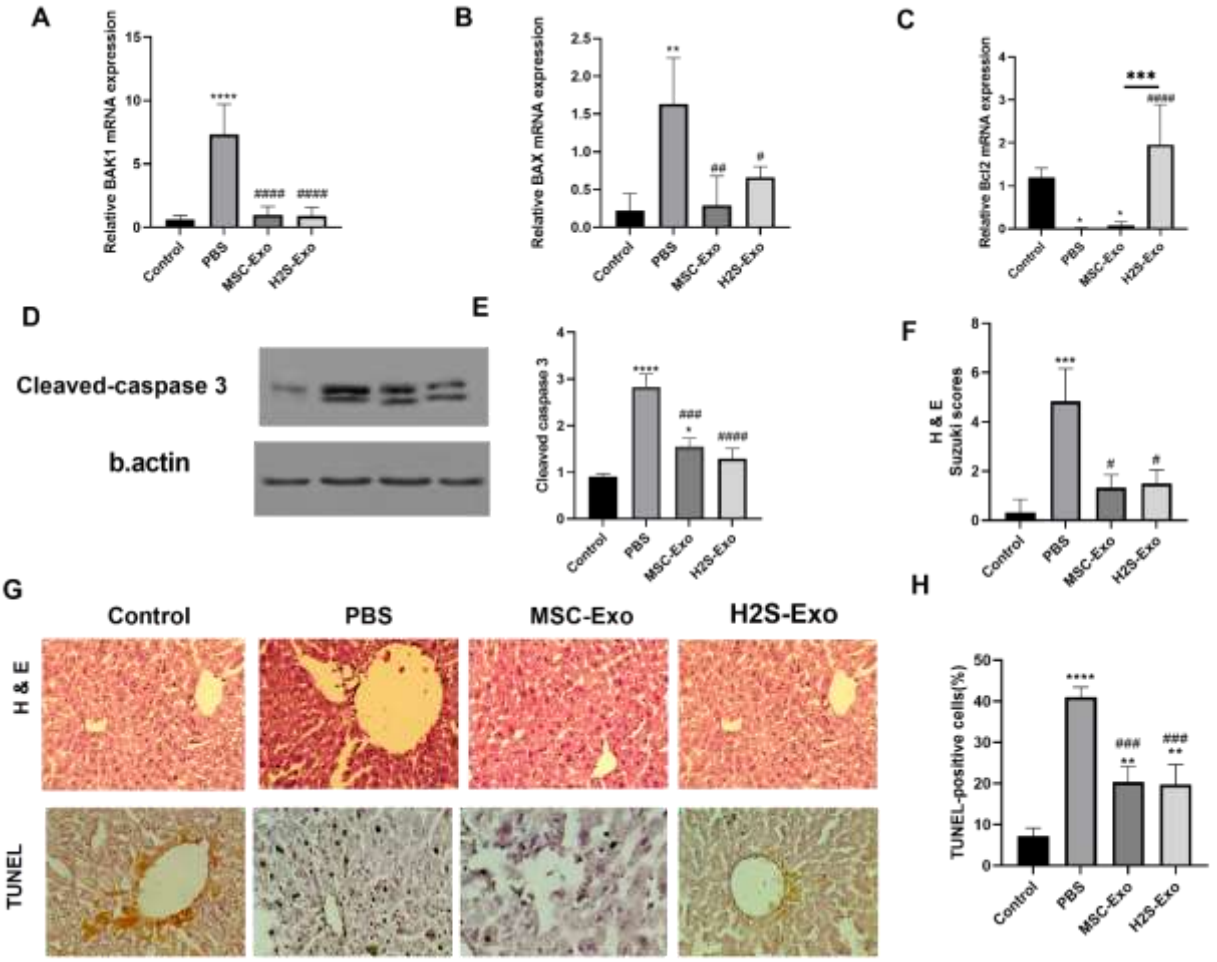

Fig. 3. MSC-Exo and H2S-Exo decreased hepatocellular apoptosis in CCL4- induced liver injury mice. (A-B) MSC-Exo and H2S-Exo administration decreased mRNA expressions of BAK1 (p-value < .0001) and BAX (p-value < .01 and p-value = .01 respectively). (C) mRNA expressions of Bcl2: (PBS and MSC-Exo group were significant as compared to control: p-value = .01 and p-value = .03 respectively). (D-E) MSC-Exo and H2S-Exo decreased cleaved caspase-3, in mice liver and MSC-Exo was significantly higher compared to control (p-value = .02). (F-G) Histopathological analysis of livers harvested 48 h after CCL4-induced injury and the severity of liver IR injury evaluated by Suzuki's histological scores. (G-H) TUNEL staining of livers and apoptotic cells was quantified and expressed as percentages of apoptotic cells among total cells. The results were analyzed using one-way ANOVA and Tukey post hoc statistical testing and expressed as mean± SD. Kruskal-Wallis tests were used for H & E staining and the results were expressed as Median + Interquartile Range. *P<0.05, **P<0.01, ***P<0.001, and ****P<0.0001 compared to control mice. #P<0.05, ## P<0.01, ### P<0.001 and ####P<0.0001 compared to PBS group.

Discussion

Lower levels of AST, ALT, T.Bili, and ALP in H2S-Exo administered mice in comparison to the MSC-Exo group was the important finding of the current study. According to our findings, MSC-Exo and H2S-Exo administration significantly reduced oxidant and cytokine levels (TNF- and IL-6) and apoptosis in liver tissue. MSC-exosomes markedly decreased pro-inflammatory cytokines and ameliorated hepatic injury. In this study, we investigated the role of NaHS-preconditioned exosomes on the hepatic inflammatory response, oxidant status, and liver tissue damage in an acute liver injury model. Based on the previous results, using one µmol NaHS achieved better outcomes in the cell viability assay and preconditioning of MSCs with NaHS exerted faster cell proliferation than non-preconditioned MSCs 48 h after incubation (18).

Most chronic and acute liver diseases occur following increased oxidant stress (25). Total oxidant status and pro-inflammatory cytokine levels are important mediators of hepatic injury (26). Oxidant stress is associated with

increased levels of ROS and pro-inflammatory cytokines (27). Pro-inflammatory cytokines play the main role in propagating the inflammatory response in acute liver injury, and the excessive increase of ROS can activate the internal pathway of apoptosis through BAK1/BAX (BCL2 Antagonist Killer1 / BCL2 Associated X) dimerization, which in turn, increases mitochondria membrane permeability, leading to its destruction and cell death (28-31).

Moreover, Ruan and colleagues showed that a single intraperitoneally injection of 30 μmol/kg NaHS (a donor of H2S), before ischemia-reperfusion modeling, could reduce Caspase-3, MDA, AST, ALT, LDH, and pathological changes in fatty liver model rats (16). In an in-vitro study, NaHS pre-treatment inhibited the production of IL-6 and TNF- in an LPS-induced hepatic injury in concentration dependent manner. Epigenetic alterations in pro-inflammatory genes due to H2S treatment may contribute to a reduction of cytokines released following stimulation with LPS (32). The present results showed that the effects of H2S-Exo on TOS and TNF-α are greater, presenting that the treatment of mesenchymal stem cells with NaHS increases the efficiency of exosomes. In contrast to the MSC-Exo group, in our investigation, H2S-Exo administration resulted in a higher decrease of oxidative and inflammatory cytokine levels (not significant).

We also found that MSC-Exo and H2S-Exo treatment attenuated the expression level of Bcl2 Antagonist/Killer 1 (BAK1), Bcl-2-associated X protein (BAX), and B-cell lymphoma 2 (Bcl2). The internal pathway of apoptosis and pro-apoptotic proteins such as BAK1/BAX are triggered by an excess intracellular ROS. Apoptotic internal pathway activation increases mitochondrial membrane permeability and contributes to cell apoptosis (33-36). The main key to the protective effect of H2S is mitochondria. Hydrogen sulfide prevents cell apoptosis by inhibiting the cleavage of caspase-3 and phosphorylation of the apoptosis-inducing MAPK p38. Also, H2S improves mitochondrial function by reducing ROS production, preserving the integrity of the mitochondrial membrane, and decreasing mitochondrial permeability (۳۷). This study revealed that MSC-Exo and H2S-Exo treatment reduced cell apoptosis through inhibition of TOS level. A low level of TOS and enhanced Bcl2 expression, inhibited BAK1/BAX dimerization and inhibited cleaved caspase-3. Importantly, our findings were emphasized by the TUNEL staining assay.

In hepatic damage, H2S therapy lowers inflammatory cytokines and cell apoptosis (15, 38). Additionally, brain ischemia-reperfusion damage is significantly reduced by H2S-modified MSC extracellular vesicles (17, 39). In this study, it was demonstrated that up-regulated expression of the apoptotic genes BAX/BAK1 and down-regulated expression of Bcl2 trigger pro-inflammatory pathways, causing hepatocytes to die. According to these results, the treatment of MSC-Exo and H2S-Exo reduced cleaved caspase-3 and significantly attenuated cell apoptosis.

We concluded that adding NaHS as an H2S donor to the cell culture medium improves the therapeutic effects of MSC exosomes by producing better results, reducing oxidant levels, and reducing pro-inflammatory cytokines. Additionally, after H2S-Exo therapy, Bcl2 expression elevated and BAK1/BAX dimerization declined.

Acknowledgements

The authors thank the Research Affairs of Jundishapur University of Medical Sciences, Ahvaz, Iran for the funding support.

Funding

This work was supported by the Research Affairs of Jundishapur University of Medical Sciences, Ahvaz, Iran (00S74, 02. October 2021).

Conflicts of Interest

The authors declare that they have no conflicts of interest.

References

1. Melgaço JG, Veloso CE, Pacheco-Moreira LF, Vitral CL, Pinto MA. Complement System as a Target for Therapies to Control Liver Regeneration/Damage in Acute Liver Failure Induced by Viral Hepatitis. Journal of Immunology Research. 2018;2018:3917032.
2. Saiman Y, Friedman S. The Role of Chemokines in Acute Liver Injury. Frontiers in Physiology. 2012;3(213).
3. Triantafyllou E, Woollard KJ, McPhail MJW, Antoniades CG, Possamai LA. The Role of Monocytes and Macrophages in Acute and Acute-on-Chronic Liver Failure. Front Immunol. 2018;9:2948.
4. Woolbright BL, Jaeschke H. Mechanisms of inflammatory liver injury and drug-induced hepatotoxicity. Current pharmacology reports. 2018;4(5):346-57.
5. Woolbright BL, Jaeschke H. The impact of sterile inflammation in acute liver injury. Journal of clinical and translational research. 2017;3(1):170.
6. Konishi T, Lentsch AB. Hepatic Ischemia/Reperfusion: Mechanisms of Tissue Injury, Repair, and Regeneration. Gene Expr. 2017;17(4):277-87.
7. Li S, Qin Q, Luo D, Pan W, Wei Y, Xu Y, et al. Hesperidin ameliorates liver ischemia/reperfusion injury via activation of the Akt pathway. Mol Med Rep. 2020;22(6):4519-30.
8. Haga H, Yan IK, Borrelli DA, Matsuda A, Parasramka M, Shukla N, et al. Extracellular vesicles from bone marrow–derived mesenchymal stem cells protect against murine hepatic ischemia/reperfusion injury. Liver Transplantation. 2017;23(6):791-803.
9. Yang R, Liu Y, Shi S. Hydrogen Sulfide Regulates Homeostasis of Mesenchymal Stem Cells and Regulatory T Cells. Journal of dental research. 2016;95(13):1445-51.
10. Hu C, Li L. Preconditioning influences mesenchymal stem cell properties in vitro and in vivo. Journal of Cellular and Molecular Medicine. 2018;22(3):1428-42.
11. Saparov A, Ogay V, Nurgozhin T, Jumabay M, Chen WCW. Preconditioning of Human Mesenchymal Stem Cells to Enhance Their Regulation of the Immune Response. Stem Cells International. 2016;2016:3924858.
12. Schäfer R, Spohn G, Baer PC. Mesenchymal stem/stromal cells in regenerative medicine: can preconditioning strategies improve therapeutic efficacy. Transfusion Medicine and Hemotherapy. 2016;43(4):256-67.
13. Waszak P, Alphonse R, Vadivel A, Ionescu L, Eaton F, Thébaud B. Preconditioning enhances the paracrine effect of mesenchymal stem cells in preventing oxygen-induced neonatal lung injury in rats. Stem cells and development. 2012;21(15):2789-97.
14. Tokuda K, Ichinose F. 0083. Hepatoprotective effects of hydrogen sulphide against acute liver failure. Intensive Care Medicine Experimental. 2014;2(1):P3.
15. Lu M, Jiang X, Tong L, Zhang F, Ma L, Dong X, et al. MicroRNA-21-Regulated Activation of the Akt Pathway Participates in the Protective Effects of H(2)S against Liver Ischemia-Reperfusion Injury. Biol Pharm Bull. 2018;41(2):229-38.
16. Ruan Z, Liang M, Deng X, Lai M, Shang L, Su X. Exogenous hydrogen sulfide protects fatty liver against ischemia–reperfusion injury by regulating endoplasmic reticulum stress-induced autophagy in macrophage through mediating the class A scavenger receptor pathway in rats. Cell Biology International. 2020;44(1):306-16.
17. Chu X, Liu D, Li T, Ke H, Xin D, Wang S, et al. Hydrogen sulfide-modified extracellular vesicles from mesenchymal stem cells for treatment of hypoxic-ischemic brain injury. Journal of Controlled Release. 2020;328:13-27.
18. J.Sameri M, Savari F, Nejad KH, Danyaei A, Mard SA. The hepato-protective effect of H2S-modified and non-modified mesenchymal stem cell exosomes on liver ischemia-reperfusion injury in mice: The role of MALAT1. Biochemical and Biophysical Research Communications. 2022.
19. Polanco JC, Scicluna BJ, Hill AF, Götz J. Extracellular vesicles isolated from the brains

of rTg4510 mice seed tau protein aggregation in a threshold-dependent manner. Journal of Biological Chemistry. 2016;291(24):12445-66.
20. Yang S, Kuang G, Zhang L, Wu S, Zhao Z, Wang B, et al. Mangiferin attenuates LPS/D-GalN-induced acute liver injury by promoting HO-1 in Kupffer cells. Frontiers in immunology. 2020;11:285.
21. Cheraghi M, Ahmadvand H, Maleki A, Babaeenezhad E, Shakiba S, Hassanzadeh F. Oxidative Stress Status and Liver Markers in Coronary Heart Disease. Reports of Biochemistry and Molecular Biology. 2019;8(1):49-55.
22. Ahmadvand H, Ghasemi Dehnoo M, Cheraghi R, Rasoulian B, Ezatpour B, Azadpour M, et al. Amelioration of Altered Serum, Liver, and Kidney Antioxidant Enzymes Activities by Sodium Selenite in Alloxan-Induced Diabetic Rats. Reports of Biochemistry and Molecular Biology. 2014;3(1):14-9.
23. Suzuki S, Toledo-Pereyra LH, Rodriguez FJ, Cejalvo D. Neutrophil infiltration as an important factor in liver ischemia and reperfusion injury. Modulating effects of FK506 and cyclosporine. Transplantation. 1993;55(6):1265-72.
24. Pan S, Liu L, Pan H, Ma Y, Wang D, Kang K, et al. Protective effects of hydroxytyrosol on liver ischemia/reperfusion injury in mice. Molecular Nutrition & Food Research. 2013;57(7):1218-27.
25. Jiang W, Tan Y, Cai M, Zhao T, Mao F, Zhang X, et al. Human Umbilical Cord MSC-Derived Exosomes Suppress the Development of CCl₄-Induced Liver Injury through Antioxidant Effect. Stem Cells International. 2018;2018:6079642.
26. Dominguez JM, Dominguez JH, Xie D, Kelly K. Human extracellular microvesicles from renal tubules reverse kidney ischemia-reperfusion injury in rats. PLoS One. 2018;13(8):e0202550.
27. Ullah H, Khan A, Baig MW, Ullah N, Ahmed N, Tipu MK, et al. Poncirin attenuates CCL4-induced liver injury through inhibition of oxidative stress and inflammatory cytokines in mice. BMC Complementary Medicine and Therapies. 2020;20(1):115.
28. Pan Y, Wang H, Tan F, Yi R, Li W, Long X, et al. Lactobacillus plantarum KFY02 enhances the prevention of CCl4-induced liver injury by transforming geniposide into genipin to increase the antioxidant capacity of mice. Journal of Functional Foods. 2020;73:104128.
29. Meng X, Tang G-Y, Liu P-H, Zhao C-J, Liu Q, Li H-B. Antioxidant activity and hepatoprotective effect of 10 medicinal herbs on CCl4-induced liver injury in mice. World journal of gastroenterology. 2020;26(37):5629.
30. Shaban NZ, El-Kot SM, Awad OM, Hafez AM, Fouad GM. The antioxidant and anti-inflammatory effects of Carica Papaya Linn. seeds extract on CCl4-induced liver injury in male rats. BMC Complementary Medicine and Therapies. 2021;21(1):1-15.
31. Sabry D, Mohamed A, Monir M, Ibrahim HA. The Effect of Mesenchymal Stem Cells Derived Microvesicles on the Treatment of Experimental CCL4 Induced Liver Fibrosis in Rats. Int J Stem Cells. 2019;12(3):400-9.
32. Rios ECS, Szczesny B, Soriano FG, Olah G, Szabo C. Hydrogen sulfide attenuates cytokine production through the modulation of chromatin remodeling. Int J Mol Med. 2015;35(6):1741-6.
33. Galluzzi L, Vitale I, Aaronson SA, Abrams JM, Adam D, Agostinis P, et al. Molecular mechanisms of cell death: recommendations of the Nomenclature Committee on Cell Death 2018. Cell Death & Differentiation. 2018;25(3):486-541.
34. Kan C, Ungelenk L, Lupp A, Dirsch O, Dahmen U. Ischemia-Reperfusion Injury in Aged Livers-The Energy Metabolism, Inflammatory Response, and Autophagy. Transplantation. 2018;102(3):368-77.
35. Yao J, Zheng J, Cai J, Zeng K, Zhou C, Zhang J, et al. Extracellular vesicles derived from human umbilical cord mesenchymal stem cells alleviate rat hepatic ischemia-reperfusion injury by suppressing oxidative stress and neutrophil inflammatory response. The FASEB Journal. 2019;33(2):1695-710.

36. De Felice F, Megiorni F, Pietrantoni I, Tini P, Lessiani G, Mastroiacovo D, et al. Sulodexide counteracts endothelial dysfunction induced by metabolic or non-metabolic stresses through activation of the autophagic program. Eur Rev Med Pharmacol Sci. 2019;23(6):2669-80.
37. Adams CM, Clark-Garvey S, Porcu P, Eischen CM. Targeting the Bcl-2 Family in B Cell Lymphoma. Frontiers in Oncology. 2019;8(636).
38. Huang X, Gao Y, Qin J, Lu S. The role of miR-34a in the hepatoprotective effect of hydrogen sulfide on ischemia/reperfusion injury in young and old rats. PloS one. 2014;9(11):e113305.
39. Zhang Q, Liu S, Li T, Yuan L, Liu H, Wang X, et al. Preconditioning of bone marrow mesenchymal stem cells with hydrogen sulfide improves their therapeutic potential. Oncotarget. 2016;7(36):58089.